Forest Canopy Heights in Amazon River Basin Forests as Estimated with the Geoscience Laser Altimeter System (GLAS)

E. H. Helmer, Research Ecologist, International Institute of Tropical Forestry, USDA Forest Service, Jardín Botánico Sur, Río Piedras, PR
M. A. Lefsky, Assistant Professor, Department of Forest, Rangeland and Watershed Stewardship, Colorado State University, Fort Collins, CO

Abstract—*Land-use change, mainly forest burning, harvest, or clearing for agriculture, may compose 15 to 40 percent of annual human-caused emissions of carbon (C) to the atmosphere. Spatially extensive data on forest C pools can validate and parameterize atmospheric and ecosystem models of those fluxes and quantify fluxes from forest change. Excellent evidence exists that light detection and ranging (lidar) waveforms can be scaled to estimate forest biomass and aboveground C pools. The Geoscience Laser Altimeter Systmem (GLAS) instrument provides satellite-based continuous return lidar data and may provide a way to inventory forest C pools globally. It was launched aboard the Ice, Cloud and Land Elevation Satellite (ICESat) on January 12, 2003. Here we explore whether GLAS data may support global inventory of forest C pools using the Amazon river basin as a study area. Forest C budgets in Amazonia are globally significant. However, globally-derived and validated Amazonian forest biomass-waveform relationships are not yet available. Consequently, here we address only vegetation canopy height. Over the Amazon basin, lands with at least 75 percent tree cover had GLAS-measured canopy heights averaging 30.48 ± 0.35 m (N = 2127). Fifty percent of measurements ranged from 25-35 m, agreeing with ground-based measurements in tierra firme forest. Lands with at least 60 percent tree cover had average canopy heights of 29.69 ± 0.10 m (N=2734). Regression-based mapping models relating waveform widths to data from maps of tree cover and elevation, or those variables plus generalized soil type, explain 36 to 47 percent of observed variation in mean vegetation canopy heights where tree cover is at least 20 percent. Finally, secondary forest age, as mapped with time series data over an area spanning three adjacent Landsat scenes in Rondonia, Brazil, was significantly related to GLAS-derived height. These results provide evidence that GLAS waveforms can contribute to global inventories of forest C pools.*

Introduction

Increases in atmospheric concentrations of CO2 and other greenhouse gases (GHGs) are projected to cause global average surface temperatures to rise 1.4 - 5.8 ºC over the next 100 years, which is rapid compared with climatic changes Earth has previously undergone (IPCC, 2001). Land-atmosphere carbon (C) fluxes are the most uncertain ones in the global atmospheric C budget, adding uncertainty to estimates of future levels and impacts of atmospheric GHGs (Prentice and others 2001; Houghton, 2003). Forest soils and woody biomass hold most of the carbon present in Earth's terrestrial biomes. Land-use change, mainly forest burning, harvest, or clearing for agriculture, may compose 15 to 40 percent of annual human-caused emissions of C to the atmosphere. Terrestrial ecosystems may absorb nearly as much C annually, with forest growth and expansion most important. Consequently, the levels, mechanisms and spatial distribution of forest land-atmosphere C fluxes are an important focus for reducing uncertainties in the global C budget (Fan and others 1998; Holland and others 1999; Pacala and others 2001; Schimel and others 2001). Spatially extensive data on forest C pools and net fluxes can parameterize and validate atmospheric and ecosystem models and quantify C fluxes from land-use change, which dominates land-atmosphere fluxes over longer periods. Such data are also necessary to monitor the differential impacts on forest ecosystems of global changes like increases in atmospheric CO^2, temperatures, nitrogen deposition, solar radiation, or cloud heights (Braswell and others 1997; Potter, 1999;

Pacala and others 2001; Schimel and others 2001; Houghton, 2003).

Forest C budgets in the Amazon river basin, the focus region of this study, are globally significant. Annual C fluxes from forest burning, clearing and regrowth in the Brazilian Amazon alone may vary from a net atmospheric C sink to a net source of about 0.2 Pg C yr –1, and logging in the region may add 5-10 percent to this estimate (Nepstad and others 1999; Houghton and others 2000). A further complication is that undisturbed forests appear to vary annually from a net C source to a sink (Saleska and others 2003). A net source of 0.2 Pg C yr-1 is equivalent to 6 to 12 percent of net C release via land-use change of 2.2 ± 0.8 Pg C yr-1 (Fan and others 1998; Pacala and others 2001). It also amounts to about 3 percent of the 6.3 ± 0.4 Pg C yr-1 of annual C emissions from fossil fuel burning and cement production during the 1990s. Yet estimates of forest C pools and fluxes in the region vary widely, and extensively-based estimates of forest biomass are probably more accurate than scaling from intensive ones (Houghton and others 2001; Saleska and others 2003). Although ground-based inventory of forest C pools is expensive, forest reflectance saturates space-based passive remote sensors at relatively low levels of aboveground biomass (Steininger, 2000; Foody and others 2003). Light detection and ranging (lidar) from satellites may, however, permit precisely located, global inventories of forest C pools in the near future. Accurate forest biomass estimates are possible with continuous return laser systems by combining waveform-measured height estimates with waveform-derived canopy-height profiles (Drake and others 2002; Lefsky and others 2002).

The Geoscience Laser Altimeter System (GLAS) is a lidar instrument that was launched aboard the Ice, Cloud, and Land Elevation satellite (ICESat) on January 12, 2003. The GLAS laser transmits short pulses (4 nano seconds) of infrared light (1064 nanometers wavelength) and visible green light (532 nanometers). Waveform returns are digitized at 15-cm intervals. As originally designed, laser pulses at 40 times per second illuminate 70-m diameter footprints that are spaced at 170-meter intervals along Earth's surface. Problems with the second laser have resulted in elliptical laser footprints of about 50 x 120 m (ICESat Land Working Group, 2004).

The goals of this study are to assess whether GLAS data have potential for monitoring forest structure across Amazonia and whether proportional forest cover may help scale GLAS-measured forest C storage from isolated waveforms to maps. Excellent evidence exists for cross-biome relationships that scale laser waveforms to forest biomass (Lefsky and others 2004). However, globally-derived and validated biomass-waveform relationships are not yet available. Consequently, in this paper we address only forest canopy height. Secondly, we estimate mapping models that relate existing geospatial datasets, like maps of proportional tree cover, to waveform height, as a rough proxy for forest C storage over an area. Thirdly, we explore the relationship between lidar-derived canopy height in Rondonia, Brazil and second growth forest as identified with Landsat data from multiple years. Excellent evidence exists for cross-biome relationships that scale laser waveforms to forest biomass (Lefsky and others 2004). However, globally-derived and validated biomass-waveform relationships are not yet available.

Consequently, in this paper we quantify only forest canopy height and mean vegetation height of partially forested land.

Methods

Lidar Waveforms and Processing

A geographic information system (GIS) coverage of Amazon basin boundaries (Mayorga and others 2002) subset GLAS waveforms collected over the region to those located within the river basin. For the basin-wide analysis, we sampled a subset of all waveforms available. Waveform processing began with characterizing background noise, which is the power that instrument noise and ambient light contribute to laser returns. Because background noise precedes and follows surface returns, its power values are the most common ones in any waveform. Consequently, fitting a Gaussian model to a histogram of power values for each waveform effectively determines a waveform-specific distribution of background noise, which yields the background noise mean and standard deviation. Multiplying the standard deviation of the background noise by a constant, in this case 5, and adding the mean noise level, estimates maximum noise level. Subtracting this maximum noise level from each waveform, and setting any resulting negative values to zero, yields a waveform of surface returns.

Both the intended and effective footprint sizes of GLAS waveforms are large enough to cause positive bias in estimates of forest canopy height on sloping land. Regressions to correct for this bias related waveform widths over presumably bare land to locationally correspondent slope indices for each study region:

$$\text{widths} = a(\text{slope index}) + b \qquad (1)$$

In Equation 1, widths is the fifth percentile of the range of waveform widths that occurs for each slope index value, which was assumed to indicate relatively bare land. All other waveform widths for a given slope index were assumed to have vegetation or other land cover above ground elevation and eliminated from the regression. Slope index is the maximum difference among all elevations in a 90-m window surrounding each waveform, which is a 3x3-pixel window for 30-m elevation data. The variables a and b are the regression slope and intercept, respectively. Elevation data derived from the Shuttle Radar Topography Mission (SRTM). Because the minimum available resolution of SRTM data outside the U.S. is 90 m, one-third of the maximum difference among pixels in the 270-m window surrounding each waveform center estimated an equivalent 90-m slope index. The resulting regression models for each study region calibrated waveform widths to remove any slope-related contribution. Corrected waveform width, widthi, was calculated from the processed waveform width (width) as follows:

$$\text{widthi} = \text{width} - \text{widths} \quad (2)$$

Mapping Models for Forest Canopy Height

We used multiple regression to estimate mapping models that relate GLAS waveform-widths, which are average heights from forested and non-forested lands for each footprint, to spatially continuous data. The mapped data included 1) percent tree cover at 500-m resolution derived from Moderate Resolution Imaging Spectroradiometer (MODIS) imagery (Hansen and others 2003), 2) elevation from SRTM digital elevation models, and 3) for the Brazilian Amazon only, generalized soil type (EMPRABA, 1981). We assumed that such mapping models might be applied to lands with at least 20 percent tree cover.

Forest Age and GLAS-Derived Canopy Height

Land-cover maps for three adjacent time series of Landsat scenes over southwestern Amazonia (Rondonia, Brazil) (Roberts and others 1998; Roberts and others 2003) provided source data to evaluate canopy heights of secondary forest of various ages. Each single date of land-cover classification distinguished between second growth forest and closed upland forest that presumably was uncut and mostly old growth. The data had a 30-m pixel size. Spatial overlays for each time series yielded land cover maps of closed upland forest and median age of second growth forest for the most recent date of Landsat imagery. Where time between Landsat scenes in a time series was more than one year, the interval midpoints were used in estimating age of second growth forest. The earliest dates for the three scene footprints were 1975, 1978 and 1986. The most recent dates were 1998 or 1999, which is about four years earlier than the dates of the GLAS waveforms. After using each time series to map old-growth forest and secondary forest age, we mosiacked the three scenes. Recoding all secondary forest to one class and all non-forest to a third class, and mapping the standard deviations of class values over 90-m windows surrounding each pixel, permitted us to identify secondary forest pixels that were only surrounded by other secondary forest pixels. For each such pixel, we then calculated an average forest age from the median forest ages over 90-m windows. We then determined which of these secondary forest pixels were locationally correspondent with the center coordinates of GLAS waveforms and used linear regression to examine the relationship between lidar-derived canopy height and secondary forest age.

Results

Amazon River Basin Closed Forest Canopy Heights

Over the entire Amazon river basin, on those lands with at least 75 percent tree cover, lidar-measured canopy heights average 30.48 ± 0.35 m (N = 2127) (table 1), and 90 percent of measurements range from 14.08 to 42.23 m. Lands with at least 60 percent tree cover over this same extent have average canopy heights of 29.69 ± 0.10 m (N=2734), with 90 percent of measurements ranging from 11.68 to 42.12 m. The distribution of canopy heights (figure 1) for closed forest canopies in the basin is slightly skewed toward taller heights; 50 percent of stands have a mean canopy height between about 25 and 35 m.

Mapping Models for Average Canopy Height

Amazon River-wide, percent tree cover and SRTM-derived elevation relate to strongly to lidar height measurements for all lands with at least 20 percent tree cover, explaining 36 percent of variation in a highly significant relationship. The same variables explain somewhat more variation, 43 percent, in lidar heights over the Brazilian Amazon (table 2). Adding soil type to elevation and tree cover as explanatory values for height over the Brazilian Amazon improved the predictive model slightly, to an R-square of 47 percent. A one-way analysis of variance (ANOVA) suggests that where tree cover is at least 60 percent, forest on podzols (spodosols) (Beinroth, 1975) is significantly shorter than closed forest on other soil types (table 3). Where tree cover is at least 75 percent, canopy height on podzols is only significantly shorter than certain soil types, including alluvial soils,

Table 1. Summary statistics for lidar-derived canopy height, SRTM-derived elevation and tree cover for lands in the Amazon River basin with at least 60 percent or 75 percent tree cover and height at least 2 m.

	Waveform height meters	Elevation meters	Tree cover percent
Tree cover at least 75%, N = 2127			
Mean	30.448	191.6	82.8
Standard deviation	8.160	170.5	4.2
Range	2.083 – 46.350	4 – 3085	75 – 100
Tree cover at least 60%, N = 2734			
Mean	29.687	198.1	80.9
Standard deviation	8.750	190.4	6.2
Range	2.050 – 46.350	1 - 3085	60 – 100

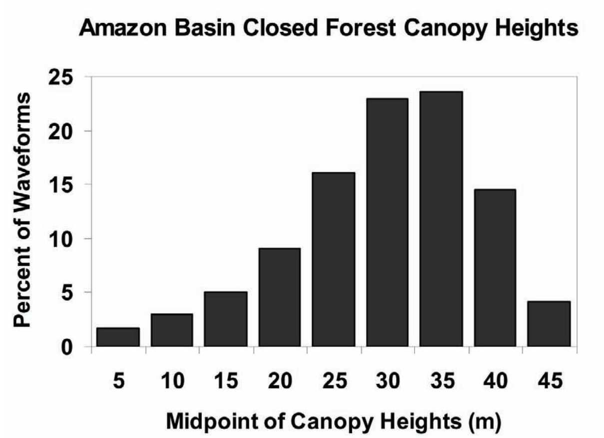

Figure 1. Frequency distribution of forest canopy heights over the Amazon River basin where tree cover is at least 75 percent and height is at least 2 m. Horizontal axis gives midpoint of heights for each bin.

Table 2. Relationships predicting height from tree cover, SRTM-derived elevation, or soil type for lands with at least 20% tree cover.

Multiple Regression Mapping Model	N	R-square	p-value
Amazon River Basin-wide			
1. HEIGHT = 1.60* + 0.350*** TREECOV + 0.00238 ELEV* – 0.0000738*** TREECOV x ELEV	3828	0.36	< 0.0001
Brazilian Amazon			
2. HEIGHT = 1.87* + 0.354*** TREECOV + 0.00420 ELEV* – 0.000154*** TREECOV x ELEV	2892	0.43	< 0.0001
3. HEIGHT = -6.22*** + 0.336*** TREECOV + 14E-5*** TREECOV x ELEV + mSOILi2	2886	0.47	<0.0001

[1] Asterisks indicate probabilities of erroneously rejecting the null hypothesis that coefficient estimates are zero, based on a two-sided t-distribution, ***p<0.0005, **p<0.005, *p<0.05.
[2] Coefficients for each soil type are given in table 3. All but four soil types had coefficient estimates that were significant at p<0.0001.

Table 3. Significant coefficient estimates for soil types in equation 3 of table 2.

Class No.	Generalized soil type	U.S. Soil Taxonomy[1]	Coefficient ± one standard error[2]
1	Alluvial soils	-	11.5 ± 2.2***
3	Cambisols	Inceptisols	14.4 ± 1.7***
5	Hydromorphic, lateriric soils	-	6.4 ± 1.4***
6	Gley soils	Inceptisols	6 ± 1.5***
9	Latosols	Oxisols	10.3 ± 1.2***
11	Podzolic soils	Ultisols	10.3 ± 1.3***
12	Deep sand soils	Entisols	9.4 ± 1.5***
13	Lithosols	Entisols	9.4 ± 1.4***
17	Planosols	Mollisols	8 ± 2.7**
19	Podzols	Spodosols	8.3 ± 1.6***

[1] Beinroth (1975) compares the Brazilian soil classification with that of the U.S. The summary does not explicitly relate hydromorphic and alluvial soils to any single U.S. soil order.
[2] Astersiks indicate probabilities of erroneously rejecting the null hypothesis that coefficient estimates are zero, based on a two-sided t-distribution, ***p<0.0005, **p<0.005, *p<0.05.

Table 4. Mean canopy heights (m) and lidar-derived elevations (m) for various soil types in the Brazilian Amazon.

Class No.	Generalized Soil Type	Mean Elevation (m)	N	Mean Height (m)	Significantly different from	Standard Deviation (m)	Range (m)
				Tree cover at least 75%			
1	Alluvial soils	17.461	13	35.394	19	4.215	29.5 - 43.4
3	Cambisols	375.530	9	35.744	19	9.878	12.2 - 45.5
5	Hydromorphic, lateriric soils	41.924	55	28.556	None	6.667	8.4 - 38.9
6	Gley soils	33.168	60	28.824	None	8.352	0.8 - 43.9
9	Latosols	122.443	767	30.809	19	8.155	1.3 - 45.6
11	Podzolic soils	184.425	383	29.732	19	8.653	0.2 - 46.4
12	Deep sand soils	246.671	34	28.985	None	7.356	14.7 - 43.1
13	Lithosols	240.907	66	30.779	None	8.637	1.7 - 45.2
19	Podzols	28.756	31	24.359	1,3,9,11	6.076	11.5 - 38
				Tree cover at least 60%			
1	Alluvial soils	17.772	15	34.983	6, 19	4.088	29.5 - 43.4
3	Cambisols	591.898	20	28.603	19	12.248	4.2 - 45.5
5	Hydromorphic, lateriric soils	41.897	66	27.849	11,6,9,19	7.701	4.5 - 41.8
6	Gley soils	33.764	84	26.608	6,19	8.912	0.8 - 43.9
9	Latosols	126.529	1000	30.192	19	8.887	0.8 - 45.9
11	Podzolic soils	193.912	467	28.968	19	8.992	0.2 - 46.4
12	Deep sand soils	256.012	43	27.027	19	8.366	7 - 43.1
13	Lithosols	250.976	79	30.342	19	8.458	1.7 - 45.2
19	Podzols	27.416	40	20.625	All	8.912	5 - 38

cambisols (inceptisols), latosols (oxisols), podzolic soils (ultisols) and lithosols (entisols). Where tree cover is at least 75 percent, the tallest forest canopies occur on alluvial soils and cambisols (table 4).

Age of Second Growth Forest and Lidar-Derived Canopy Heights

After excluding areas of mixed land cover in 90-m windows, secondary forest age in 1998-99 was significantly related to lidar-derived height in 2003 ($p < 0.005$) (figure 2). The relationship between median age of second growth forest in 1998-99 and lidar-derived canopy height in 2003 is Log10(age) = 0.349 + 0.0161(height) (R-square = 0.40, N = 22, $p < 0.005$). Assuming that all second growth forest was 4 yr older in 2003, the following equation results: Log10(age) = 0.778 + 0.0905(height) (R-square = 0.39, N = 22, $p < 0.005$).

Discussion

Canopy height measurements from GLAS agree with previous ground-based studies in the Amazon region. In Paragominas, Pará, Brazil, upland seasonal evergreen old-growth forest on latosols (oxisols) and podzolic soils (ultisols), the most common soil types in the region, are 2535 m tall (Uhl and others 1988). They correspond well with the average closed canopy height of about 30 m from

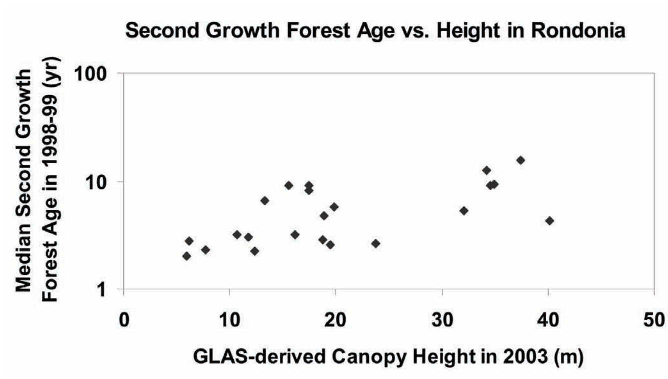

Figure 2. Relationship between median age of second growth forest in 1998-99 and lidar-derived canopy height in 2003.

GLAS measurements and a distribution of canopy heights in which 50 percent of measurements range from 25-35 m. The average canopy height of forest on podzols (spodosols) of 24 m, with 90 percent of measurements between 12 and 33 m, also corresponds well with forest height observed on those soils of 20-30 m for Caatinga forest and 5-10 m for Bana forest (Kauffman and others 1988).

Regression-based mapping models relating GLAS-derived mean canopy heights to data from maps of tree cover and elevation explain 36 to 47 percent of observed variation in waveform widths over the Amazon basin and the Brazilian Amazon. Insofar as GLAS-derived mean heights over lands with 20 percent or more tree cover serve as a proxy for forest-related C storage over a given 500m pixel, the geospatial layers that we used can contribute to scaling estimates of forest C storage globally. Based on results in the Brazilian Amazon, global geospatial data on soil types might further improve such mapping models. Identifying soil type with the less generalize 70- or 249class versions of the Brazilian soils map might also enable soil type to explain more of the variability in waveform width. Clay content of terra firme forest latosols, which is related to several soils fertility parameters, explained one-third of the variability in biomass of those forests (Laurance and others 1999).

Finally, the significance of the relationship between second growth forest age in 1998-99 and GLAS-derived canopy heights in 2003 demonstrates that GLAS data are sensitive to age-related differences in forest canopy height. This result provides further evidence that GLAS waveforms can contribute to global inventories of forest C pools.

Conclusions

Apparently valid height estimates of closed forest canopies are derivable from GLAS waveforms for both the Amazon River basin and by generalized soil type for the Brazilian Amazon. In addition, maps of proportional tree cover, elevation, and soils are likely to contribute to scaling GLAS-based estimates of forest C pools to spatially continuous data.

Acknowledgments

We thank the Earth Observing System (EOS)-Webster, at the University of New Hampshire, through which we obtained the generalized soils map for the Brazilian Amazon, and NASA's Large Basin Amazonia (LBA) program, through which we obtained geospatial data for the Amazon River basin boundaries (courtesy of the University of Washington Department of Oceanography), and the time series of land cover for the Rondonia study area (courtesy of Dar Roberts). We obtained MODIS tree cover data from the University of Maryland's Global Land Cover Facility. This research was conducted with cooperation from the University of Puerto Rico.

References

Beinroth, F. H. (1975). Relationship between U.S. soil taxonomy, the Brazilian soil classification system, and FAO/UNESCO soil units. In Soil management in tropical America (E. Bornemisza, and A. Alvarado, Eds.). University Consortium on Soils of the Tropics and the Soil Science Department, North Carolina State University, Raleigh, NC, Cali, Columbia, pp. 92-108.

Braswell, B. H., Schimel, D. S., Linder, E., and Moore, B., III. (1997). The Response of Global Terrestrial Ecosystems to Interannual Temperature Variability. Science 278: 870-873.

Drake, J. B., Dubayah, R. O., Clark, D. B., Knox, R. G., Blair, J. B., Hofton, M. A., Chazdon, R. L., Weishampel, J. F., and Prince, S. (2002). Estimation of tropical forest structural characteristics using large-footprint lidar. Remote Sensing of Environment 79:305-319.

EMPRABA. (1981). Mapa de solos do Brazil, Empresa Brasileña de Investigaciones Agropecuarias. Instituto Brasileiro de Geografia e Estatística, digitized by N. Bliss in 1992, USGS EROS Data Center, Sioux Falls, SD.

Fan, S., Gloor, M., Mahlman, J., Pacala, S., Sarmiento, J., Takahashi, T., and Tans, P. (1998). A Large Terrestrial Carbon Sink in North America Implied by Atmospheric and Oceanic Carbon Dioxide Data and Models. Science 282:442-446.

Foody, G. M., Boyd, D. S., and Cutler, M. E. J. (2003). Predictive relations of tropical forest biomass from Landsat TM data and their transferability between regions. Remote Sensing of Environment 85:463-474.

Hansen, M., DeFries, R., Townshend, J. R., Carroll, M., Dimiceli, C., and Sohlberg, R. (2003). 500m MODIS Vegetation Continuous Fields: Tree Cover. Global Land Cover Facility, The University of Maryland, College Park, MD.

Holland, E. A., Brown;, S., Potter, C. S., Klooster;, S. A., Fan, S., Gloor, M., Mahlman, J., Pacala, S., Sarmiento, J., Takahashi, T., and Tans;, P. (1999). North American Carbon Sink. Science 283:1815a.

Houghton, R. (2003). Revised estimates of the annual net flux of carbon to the atmosphere from changes in land use and land management 1850 - 2000. Tellus 55B:378-390.

Houghton, R. A., Lawrence, K. T., Hackler, J. L., and Brown, S. (2001). The spatial distribution of forest biomass in the Brazilian Amazon: a comparison of estimates. Global Change Biology 2001:731-746.

Houghton, R. A., Skole, D. L., Nobre, C. A., Hackler, J. L., Lawrence, K. T., and Chomentowski, W. H. (2000). Annual fluxes of carbon from deforestation and regrowth in the Brazilian Amazon. Nature 403:301-304.

IPCC. (2001). Summary for policymakers. In Climate change 2001: the scientific basis (D. Yihui, Ed.), Climate Change 2001. Cambridge University Press, Cambridge, pp. 1-20.

Kauffman, J. B., Uhl, C., and Cummings, D. L. (1988). Fire in Venezuelan Amazon 1: Fuel biomass and fire chemistry in the evergreen rainforest of Venezuela. Oikos 53.

Laurance, W. F., Fearnside, P. M., Laurance, S. G., Delamonica, P., Lovejoy, T. E., Rankin-de Merona, J. M., Chambers, J. Q., and Gascon, C. (1999). Relationship between soils and Amazon forest biomass: a landscape-scale study. Forest Ecology and Management 118:127-138.

Lefsky, M. A., Cohen, W. B., Parker, G. G., and Harding, D. J. (2002). Lidar remote sensing for ecosystem studies. Bioscience 52:19-30.

Lefsky, M. A., Hudak, A. T., Cohen, W. B., and Acker, S. A. (2004). Geographic variability in lidar predictions of forest stand structure in the Pacific Northwest. Remote Sensing of Environment In press.

Mayorga, E., Logsdon, M. G., and Miller, A. (2002). Estimating cell-to-cell land surface flow paths from digital channel networks, with an application to the Amazon basin. University of Washington, School of Oceanography, Box 355351, Seattle, WA 98195.

Nepstad, D. C., Veríssimo, A., Alencar, A., Nobre, C. A., Lima, E., Lefebvre, P., Schlesinger, P., Potter, C. S., Moutinho, P., Mendoza, E., Cochrane, M., and Brooks, V. (1999). Large-scale impoverishment of Amazonian forests by logging and fire. Nature 398:505-508.

Pacala, S. W., Hurtt, G. C., Baker, D., Peylin, P., Houghton, R. A., Birdsey, R. A., Heath, L., Sundquist, E. T., Stallard, R. F., Ciais, P., Moorcroft, P., Caspersen, J. P., Shevliakova, E., Moore, B., Kohlmaier, G., Holland, E., Gloor, M., Harmon, M. E., Fan, S.-M., Sarmiento, J. L., Goodale, C. L., Schimel, D., and Field, C. B. (2001). Consistent Land- and Atmosphere-Based U.S. Carbon Sink Estimates. Science 292:2316-2320.

Potter, C. S. (1999). Terrestrial biomass and the effects of deforestation on the global carbon cycle. Bioscience 49:769-778.

Prentice, I. C., Farquhar, G. D., Fasham, M., Goulden, M., Heimann, M., Jaramillo, V., Kheshgi, H., Le Quéré, C., Scholes, R., and Wallace, D. (2001). Ch. 3 The carbon cycle and atmospheric carbon dioxide. In Climate change 2001: the scientific basis (D. Yihui, Ed.), Climate Change 2001. Cambridge Univ. Press, Cambridge, pp. 183-237.

Roberts, D. A., Batista, G., Pereira, J., Waller, E., and Nelson, B. (1998). Change Identification using Multitemporal Spectral Mixture Analysis: Applications in Eastern Amazonia. In Remote Sensing Change Detection: Environmental Monitoring Applications and Methods (R. Lunetta, Ed.). Ann Arbor Press, Ann Arbor, MI, pp. 137-161.

Roberts, D. A., Numata, I., Holmes, K. W., Batista, G., Krug, T., and Chadwick, O. A. (2003). Large area mapping of land-cover changes in Rondonia using multitemporal spectral mixture analysis and decision tree classifiers. Journal of Geophysical Research 107:40-1 - 40-18.

Saleska, S. R., Miller, S. D., Matross, D. M., Goulden, M. L., Wofsy, S. C., da Rocha, H. R., de Camargo, P. B., Crill, P., Daube, B. C., de Freitas, H. C., Hutyra, L., Keller, M., Kirchhoff, V., Menton, M., Munger, J. W., Pyle, E. H., Rice, A. H., and Silva, H. (2003). Carbon in Amazon Forests: Unexpected Seasonal Fluxes and Disturbance-Induced Losses. Science 302:1554-1557.

Schimel, D. S., House, J. I., Hibbard, K. A., Bousquet, P., Ciais, P., Peyline, P., Braswell, B., Apps, M., Baker, D., Bondeau, A., Canadell, J., Churkina, G., Cramer, W., Denning, A., Field, C., Friedlingstein, P., Goodale, C., Heimann, M., Houghton, R., Melillo, J., Moore, B. I., Murdiyarso, D., Noble, I., Pacala, S., Prentice, I. C., Raupach, M., Rayner, P., Scholes, R., Steffen, W., and Wirth, C. (2001). Recent patterns and mechanisms of carbon exchange by terrestrial ecosystems. Nature 414:169-172.

Steininger, M. K. (2000). Satellite estimation of tropical secondary forest above-ground biomass: data from Brazil and Bolivia. International Journal of Remote Sensing 21:1139-1157.

Uhl, C., Buschbackher, R., and Serrão, A. S. (1988). Abandoned pastures in eastern Amazonia I. patterns of plant succession. Journal of Ecology 75:663-681.